Eclipsing light curves for accretion flows around a rotating black hole and atmospheric effects of the companion star

Rohta Takahashi[1]

[1] Cosmic Radiation Laboratory, the Institute of Physical and Chemical Research (RIKEN)
2-1 Hirosawa, Wako, Saitama 351-0198, Japan
E-mail: rohta@riken.jp

Abstract

We calculate eclipsing light curves for accretion flows around a rotating black hole taking into account the atmospheric effects of the companion star such as the atmospheric absorption and scattering effects. By using the solar-type atmospheric model, we have taken into account the atmospheric effects of the companion star, such as the photoionization by HI and HeI. We found that the eclipsing light curves observed at 1 keV possibly contain the information of the black hole spin. However, in our atmospheric model, the effects of the atmosphere are much larger than the effects of the black hole spin. Therefore, even in the case that the light curves contain the information of the black hole spin, it may be difficult to extract the information of the black hole spin if we do not have the realistic atmospheric profiles, such as the temperature, and the number densities for several elements. If the light curves of the occultation events of the black hole binaries are detected by MAXI, the light curves contain the information of the atmosphere of the companion star and, possibly, a black hole's spin. Takahashi & Watarai (2007) also contains other details of the present study.

Key words: workshop: proceedings — LaTeX2.09: style file — instructions

1. Introduction

In order to obtain physical information of the strong gravity region in the vicinity of black holes, direct imaging of a black hole is an extremely promising method. The emission from the vicinity of the event horizon contains information about the physical parameters of a black hole. Since the apparent shapes of the black hole shadows and the appearances of the circular orbit around the black hole are deformed by the effects of the black hole's rotation and charge (e.g. Cunningham & Bardeen 1972, Bardeen 1973, Takahashi 2004, 2005), the size and the position of the most luminous parts generally existing in the vicinity of the shadow depend on the physical parameters of black holes.

In general, methods for probing strong-field gravity near supermassive black holes or stellar-mass black holes are quite limited. Although the past VLBI observations give the images of the galactic centers with the spatial resolution within 100 Schwarzschild radii (e.g., for Sgr A*, Shen et al. 2005, for M87, Junor, Biretta & Livio 1999), the direct mapping of the shadows of both supermassive and stellar-mass black holes has not been performed so far. Several future interferometers have plans to image the shadows around massive black holes: e.g. VSOP-2 for radio (Hirabayashi et al. 2005). While these planned interferometers will image the massive black hole, direct imaging of the stellar-mass black holes are difficult because the apparent size of the black hole shadow is extremely small. Even with the future planned radio or X-ray interferometer, the direct mapping of the shadow of the stellar-mass black hole is practically impossible. However, if the stellar-mass black hole in the binary system is occulted by its companion star, the eclipsing light curves give the direct information for the spatial distribution of the brightness patterns of the accretion flows around the black hole. This is the primary motivation of the present study.

In the present study, we study the method to investigate the physical information included in the strong-gravity region around the black hole by light-curve analysis for an accretion disc around a black hole occulted by its companion star. The basic idea for the eclipsing light curve analysis was first proposed by Fukue (1987). Watarai, Takahashi & Fukue (2005) investigated the eclipsing light curves for the supercritical accretion flows which may be suggested as the accretion flow model for some X-ray black-hole binaries. In principle, light curves obtained at the time of eclipsing have information about the black hole if the region around the black hole is optically thin. However, the real observational data of the eclipsing light curves may contain the addi-

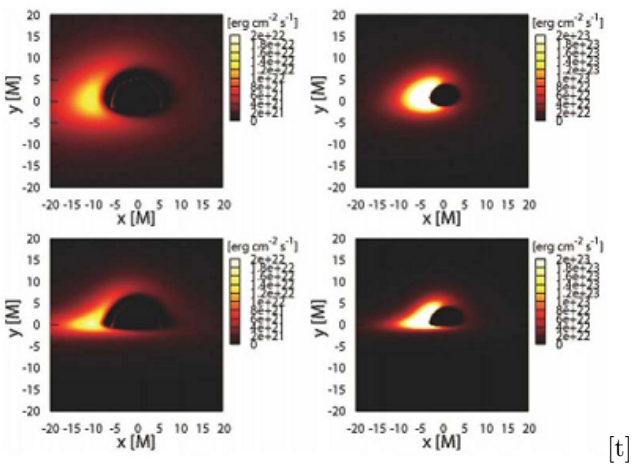

Fig. 1. Bolometric flux distribution (erg cm^{-2} s^{-1}) for black-hole spins of $a/M = 0$ (*left panels*) and 1 (*right panels*), and inclination angles of $i = 60°$ (*top panels*) and $80°$ (*bottom panels*). The relativistic standard discs are adopted. The inner edge of the accretion disc is assumed to be the marginally stable circular orbit. For non-rotating black holes, indirect images can be seen in the region within the inner stable circular orbit. The flux distributions are asymmetric due to the disc rotation and the frame-dragging effects. The shapes of the shadows casted by the black holes are asymmetric due to frame-dragging effects around the rotating black holes.

tional effects which are not sometimes simple. One of such effects is the atmospheric effects of the companion star. Recently, Pietsch et al. (2006) give the observational data of the eclipsing light curves for the X-ray binary M33 X-7 detected by *Chandra*. In soft X-ray, the atmospheric effects in the companion star may vanish the relativistic effects in the eclipsing light curves. In other words, the eclipsing light curves also contain the information of the atmosphere of the companion star. Thus, the eclipsing light curve analysis will be used for the investigation of the atmosphere of the companion star. In the present study, we also investigate the companion star's atmospheric effects in the eclipsing light curves of the black-hole binaries, and compare these effects with the effects of the black hole's rotation.

2. Eclipsing Light Curves without Atmospheric Effects

In order to calculate a light curve during an eclipse, some assumptions were required. In the present study, we assume the relativistic standard disc (Novikov & Thorne 1973, Page & Thorne 1974) at equatorial plane. Based on this model, the radial profile of the effective temperature of the accretion flow can be calculated. Then, at each radius, we assume the black body spectrum with the effective temperature calculated from the relativistic standard accretion disc model.

The calculation method for the observed spectrum of the emission in the Kerr metric is established (e.g. Cunningham & Bardeen 1973). At each light ray, the observed specific intensity, $I_{\nu_{\rm obs}}$ [erg s^{-1} cm^{-2} str^{-1} Hz^{-1}], of the accretion disc observed at the photon frequency $\nu_{\rm obs}$ is calculated as $I_{\nu_{\rm obs}} = g^3 I_{\nu_{\rm rest}}$, where $\nu_{\rm rest}$ is the photon frequency measured in the local rest frame of the accretion flow, $T_{\rm eff}$ is the temperature of the relativistic standard accretion disc at the radius where the light ray intersects, $I_{\nu_{\rm rest}}$ is the specific intensity measured at the local rest frame of the accretion disc, and g is the frequency ratio defined $g = \nu_{\rm obs}/\nu_{\rm rest}$. The frequency ratio g is calculated same as Cunningham & Bardeen (1973). In this study, we assume $I_{\nu_{\rm rest}}$ is the black body spectrum with the effective temperature at the radius where the light ray intersects, i.e. $I_{\nu_{\rm rest}} = B_{\nu_{\rm rest}}(T)$, where T is the temperature of the accretion disc. By using the relation $d\nu_{\rm obs} = g d\nu_{\rm rest}$ and the assumption of the isotropic radiation at the local rest frame of the accretion disc, the observed flux $F_{\rm obs}$ [erg s^{-1} cm^{-2}] is calculated as $F_{\rm obs} = (1/d^2)\int g I_{\nu_{\rm obs}} d\nu_{\rm obs} = (1/d^2)\int g^4 I_{\nu_{\rm rest}} d\nu_{\rm rest}$ where d is the distance to the accretion disc. By integrating the observed flux in x-y plane, we can calculate the observed bolometric lumi-

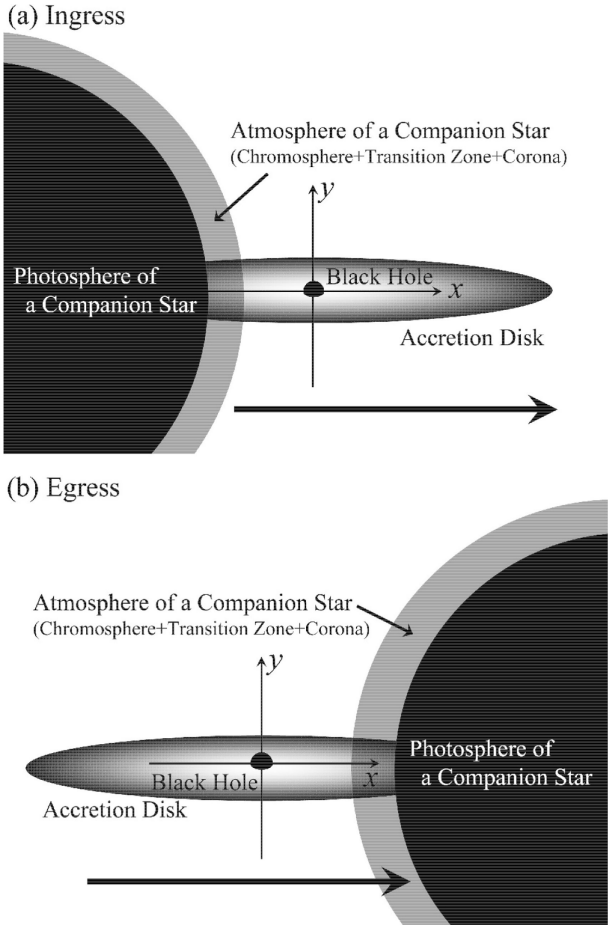

Fig. 2. Schematic diagrams for the eclipsing black-hole binaries when the ingress (*top panel*) and the egress (*bottom panel*).

nosity $L_{\rm bol}$ [erg s^{-1}]. On the other hand, the observed flux at the observed photon frequency $\nu_{\rm obs}$, $F^{\rm obs}_{\nu_{\rm obs}}$ [erg s^{-1} cm^{-2} Hz^{-1}], is calculated by using the delta-function as $F_{\nu_{\rm obs}} = (1/d^2)\int g^4 I_{\nu_{\rm rest}}\delta(\nu_{\rm obs} - g\nu_{\rm rest})d\nu_{\rm rest}$. By integrating the flux in x-y plane, the luminosity at the observed frequency $\nu_{\rm obs}$, $L_{\nu_{\rm obs}}$ [erg s^{-1} Hz^{-1}] is calculated. The luminosity are calculated by the ray-tracing method, which is commonly used in the past studies (e.g. Fukue & Yokoyama 1988, Takahashi 2004).

For all calculations in the present study, we assume a black hole mass of $10M_\odot$ and mass accretion rate of $1\dot{M}_{\rm Edd}$, and the disc thickness is neglected. Here $\dot{M}_{\rm Edd}$ is the Eddington mass accretion rate defined as $\dot{M}_{\rm Edd} \equiv L_{\rm Edd}/c^2 = 1.4\times10^{17}(M/M_\odot)$ [g/s] where $L_{\rm Edd}$ is the Eddington luminosity (e.g. Kato, Fukue & Mineshige 1998). Also, we implicitly assume that the binary system has a relatively high inclination angle, $i > 60^\circ$. In figure 1, we show examples of the spatial distribution of the observed flux of the accretion flows in the vicinity of the black holes. For all panels of figure 1, the mass center of the black hole is at the center of the image. The width and the height of the images in figure 1 are both 20 M where M is the gravitational radius and 1 M corresponds to 0.5 Schwarzschild radius. We define x-axis and y-axis as the horizontal line and the vertical line crossing at the center of the each image of figure 1. In figure 1, the position of the mass center of the black hole is at $(x,\ y) = (0,\ 0)$, and the displayed region is -10 $[M]< x < 10$ $[M]$ and -10 $[M]< y < 10$ $[M]$. Based on the calculations of the observed luminosity described above, we calculate the eclipsing light curves.

In figure 2, we show the schematic diagrams for the eclipsing black-hole binaries when the ingress (*top panel*) and the egress (*bottom panel*). We also plot x-axis and y-axis in panels of figure 2. When the ingress and the egress phases described in figure 2, the companion star is crossing the line of sight between the observer and the black hole binary along the direction of x-axis. Since the size of the companion star is generally much larger than the emission region around the black hole, we assume the carve of the stellar surface as the straight line in our calculations. Although in our calculations the brightness profiles of the accretion disc are calculated within $r < 200$ $[M]$, the light curves are calculated in the range of -60 $[M]< x < 60$ $[M]$. That is, in terms of the range in y-axis direction, we use the brightness profile of the disc in the range of -200 $[M]< y < 200$ $[M]$, but the brightness profiles of the accretion disc are given within $r < 200$ $[M]$.

3. Atmospheric Model of Companion Star and Eclipsing Light Curves with Atmospheric Effects

In the present study, we use the atmospheric model calculated for the solar atmosphere (Daw et al. 1995, Fontenla et al. 1993, Gabriel 1976). In the top panel of figure 3, we plot HI number density $N_{\rm HI}$ [cm^{-3}] (*solid line*) and temperature T [K] (*dashed line*) of the adopted atmosphere model. Here, H [km] denote the height above the photosphere. Temperature of the atmosphere suddenly increase and the number density decrease in the transition zone between the lower chromosphere ($\sim 10^{3-4}$ [K]) and the upper corona ($\sim 10^6$ [K]). The two separate temperatures of HI correspond to two stable regions of the cooling function of HI (e.g. chapter 6 in Spitzer 1978).

Table 1. Cross sections [cm^2] for photoionization absorption due to HI, HeI, HeII and Compton scattering in X-ray of 0.1 keV, 1 keV and 10 keV.

	0.1 keV	1 keV	10 keV
$\sigma_{\rm HI}$	1.9×10^{-20}	1.1×10^{-23}	4.5×10^{-27}
$\sigma_{\rm HeI}$	3.9×10^{-19}	3.4×10^{-22}	1.4×10^{-25}
$\sigma_{\rm HeII}$	3.0×10^{-19}	2.7×10^{-22}	1.3×10^{-25}
$\sigma_{\rm Comp}$	1.4×10^{-25}	1.3×10^{-25}	6.4×10^{-25}

In figure 4, we show the schematic diagrams for the observer, the eclipsing black-hole binaries, the companion star with its atmosphere and the light ray penetrating the atmosphere. Here, the light ray penetrates the atmosphere with the length of $2\ell_{\rm max}$. $H_{\rm max}$ is the length from the center of the companion star to the maximum height of the atmosphere, and H is the length between the center of the companion star and the point where the light ray penetrate the atmosphere. The optical depth, $\tau(\nu)$, in the atmosphere can be calculated as

$$\tau(\nu) = \int d\ell\ (\sigma_{\rm abs}N_{\rm abs} + \sigma_{\rm sca}N_{\rm sca}), \qquad (1)$$

where $\sigma_{\rm abs}$ and $\sigma_{\rm sca}$ are cross sections of the absorption and scattering, respectively, and $N_{\rm abs}$ and $N_{\rm sca}$ are the number densities of the absorber and the scattering medium, respectively. The integrations are performed along the atmosphere of the companion star in the line of sight.

In soft X-ray band, the photoionization absorption by hydrogen and helium contribute to opacity. The photoionization absorption cross sections of HI, HeI and HeII in soft X-ray are summarized in table 1. We also calculate the Compton scattering cross section in the same table. Since for 0.1 keV and 1 keV the scattering cross section is significantly lower than the absorption cross sections, we can neglect the effects of the Compton scatterings. On the other hand, for 10 keV the scattering effects are dominated. In this case, we only take into account the out-going photons as the scattering effects for simplicity. We see that the photoionization absorption cross sections of HI, HeI and HeII are comparable in soft X-ray. Calculations by Fontenla et al (1993) shows that the number density of HeII, $N_{\rm HeII}$, is significantly lower,

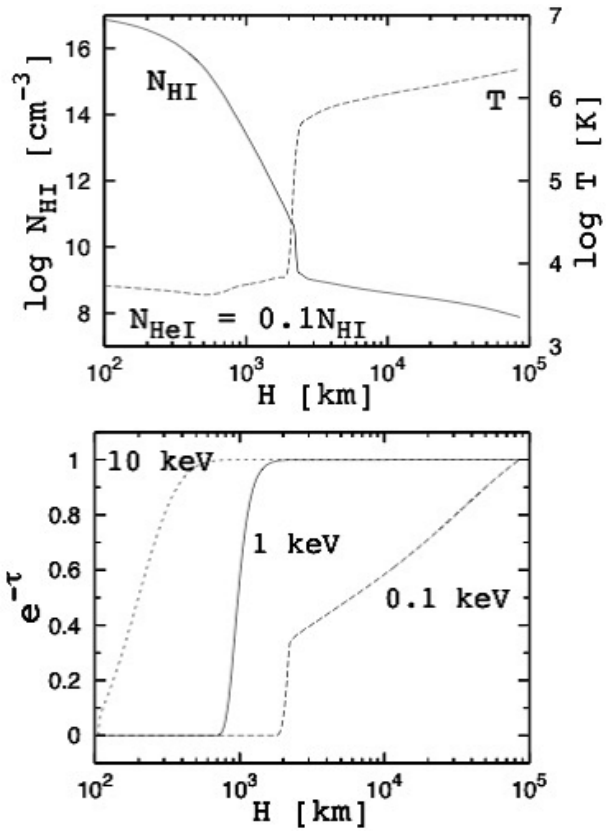

Fig. 3. HI number density $N_{\rm HI}$ [cm^{-3}] (*solid line*) and temperature T [K] (*dashed line*) of the adopted atmosphere model (*top panel*). The atmosphere model has been constructed for the solar atmosphere (Daw et al. 1995). The number density of HeI, $N_{\rm HeI}$, is assumed to be $N_{\rm HeI} = 0.1 N_{\rm HI}$. The corresponding transparency ratio, $e^{-\tau}$, of the modeled atmosphere (*bottom panel*) for X-ray: 0.1 keV (*long dashed line*), 1 keV (*solid line*), 10 keV (*short dashed line*). Here, τ is the optical depth of the photoionization absorption by HI and HeII.

e.g. by order 4, than that of HI, $N_{\rm HI}$, in the solar atmosphere, i.e. $N_{\rm HeII} \ll N_{\rm HI}$, and the number density of HeI is lower by about order 1 than that of HI through the atmosphere, i.e. $N_{\rm HeI} \sim N_{\rm HI}$. Therefore, in the present study, we neglect the scattering effects in the atmosphere for 0.1 keV and the absorption by HeII for 0.1 keV, 1 keV and 10 keV. Then, we calculate the optical depth in the atmosphere as

$$\tau(\nu) = 2\int_0^{\ell_{\rm max}} d\ell\, (\sigma_{\rm HI} N_{\rm HI} + \sigma_{\rm HeI} N_{\rm HeI} + \sigma_{\rm Comp} N_e), \quad (2)$$

where $\ell_{\rm max} = (H_{\rm max}^2 - H^2)^{1/2}$, $H_{\rm max}$ is set to 10^5 [km], the number density of electrons N_e is calculated only in the photosphere based on numerical table given by Fontenla et al. (1993). However, according to Fontenla et al. (1993) the number density of electrons in the atmosphere is lower than that of HI by factor 3-4 in the almost region of photosphere, then the scattering effects are negligible in the photosphere. Near the transition

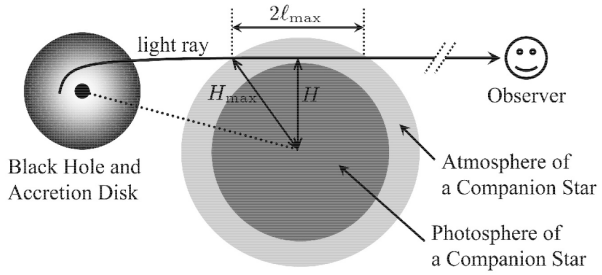

Fig. 4. Schematic diagrams for the observer, the eclipsing black-hole binaries, the companion star with its atmosphere and the light ray penetrating the atmosphere. Here, the light ray penetrate the atmosphere with the distance $2\ell_{\rm max}$. $H_{\rm max}$ is the distance from the center of the companion star to the maximum height of the atmosphere, and H is the distance between the center of the companion star and the point where the light ray penetrate the atmosphere.

zone, the number density of the electron is lower than that of HI within factor 1, and for cases of 10 keV the scattering effects contribute to the optical depth. By using the optical depth calculated above, we solve the radiative transfer equation along the atmosphere in the line of sight. The brightness decreases along the light rays in the atmosphere by the exponential of the optical depth.

By using the optical depth τ calculated above, the observed luminosity with the atmospheric effects is calculated by multiplying the factor $e^{-\tau(\nu_{\rm obs})}$ to the observed luminosity without the effects of the atmospheric effects. The observed luminosity without the atmospheric effects corresponds to the case of $\tau = 0$. Since the distance between the accretion disc and the atmosphere of the companion star is very large, here we evaluate the optical depth τ at the observed photon frequency $\nu_{\rm obs}$. In the bottom panel of figure 3, we show the corresponding transparency ratio, $e^{-\tau}$, of the modeled atmosphere for X-ray: 0.1 keV (*long dashed line*), 1 keV (*solid line*), 10 keV (*short dashed line*). In the cases of 1 keV and 10 keV, while the lines in the corona are optically thin, the photoionization absorption is effective in the photosphere. By using the optical depths calculated as figure 3, we calculate the eclipsing light curves with the atmospheric effects of the companion star in later section.

4. Black Hole Shadows with the Atmospheric Effects

We first calculate the images of the black hole shadows with absorption effects in the atmosphere of the companion star. In figure 5, we show images of black hole shadows when ingress at the observed frequency of 1 keV for cases with no absorption effects (*top panels*) and atmospheric photoionization absorptions (*bottom panels*). We assume the mass of the companion star to be 1 $M_\odot$. The size of each image is same as figure 1, i.e. -20 $[M] < x <$20

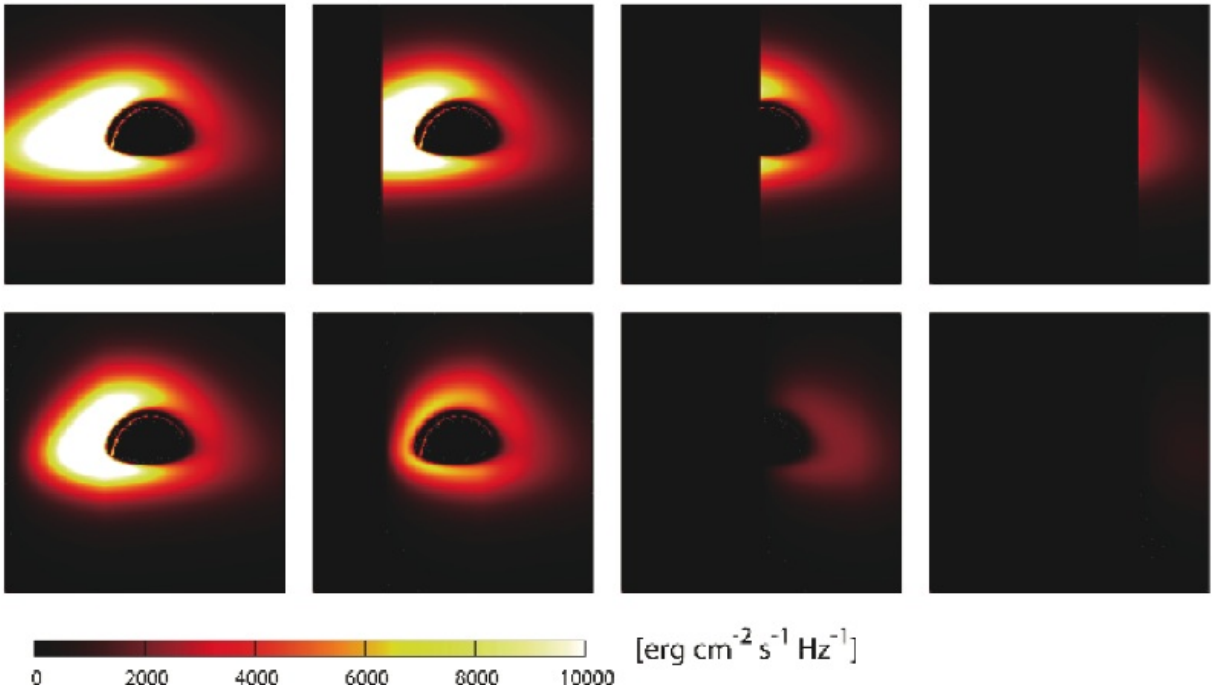

Fig. 5. Images of black hole shadows with $a/M = 0.5$ when ingress at the observed frequency of 1 keV for cases with no absorption effects (*top panels*) and atmospheric absorptions (*bottom panels*). The size of each image is same as figure 1, i.e. $-20 < x/M < 20$ and $-20 < y/M < 20$. For no absorption case for top panels, the edges of the companion star are located at -20, -10, 0 and 10 in units of M (*left to right*). For the absorption case for bottom panels, we define these edges as positions with $\tau(\nu) = 7$.

$[M]$ and -20 $[M] < y < 20$ $[M]$. For no absorption case for top panels, the edges of the companion star are located at -20, -10, 0 and 10 in units of M (*left to right*). For the cases with the atmospheric effects (*bottom panels*), we define these edges as positions with $\tau(\nu) = 7$. We can see that the brightness around the black hole shadow are decreased by the photoionization absorption in the atmosphere. In addition to the decrease of the absolute values of the brightness, the clear edges of the companion star which can be seen for no absorption cases are smeared out by the absorption effects. This is because the effective region with absorption effects is comparable to the size of X-ray emitting regions. We next calculate the eclipsing light curves with effects of the photoionization absorption. In figure 6, we show normalized light curves with (*thick lines*) and without (*thin lines*) the atmospheric effects of the companion star. The observed energy is set to be 1 keV in figure 6. The black hole spins are $a/M = 0$ (*solid lines*) and 1 (*dotted lines*), and the observed inclination angles with respect to the rotation axis of the accretion disc are $i = 60°$ (*top panels*) and 80° (*bottom panels*). While the normalization light curves with no absorption effects largely change in a short time when the most luminous parts of the accretion disc are occulted or unocculted by the sharp edge of the companion star, the normalization light curves with absorption effects gradually decrease or increase compared to the cases with no absorption effects. This is because the atmosphere of the companion star absorb some fraction of X-ray photons gradually before the most luminous part of the accretion disc is completely occulted or unocculted. In other words, the width of the absorption region which causes the gradual changes of the X-ray brightness of the accretion disc is comparable to size of the luminous parts of the accretion disc as denoted above.

Since the size of the most luminous parts of the accretion disc depends on the black hole spin, the crossing timescale of the companion star along the most luminous parts of the accretion disc can be one of the key physical quantities which distinguish the cases of rapidly rotating black holes and the cases of no rotating black hole. But these effects are generally smeared out by the atmospheric effects of the companion star at some fraction. In our calculations assuming the solar atmosphere, the atmospheric absorption can not completely smeared out the difference between the cases of rapidly rotating black holes and the cases of no rotating black hole. Then, the observed eclipsing light curves at 1 keV with the atmospheric effects of the companion star possibly contain the information of the black hole spin. However, since the effects of the atmosphere is larger than the effects of the spin, only when we have the reliable atmospheric model, we can determine the black hole spin from the

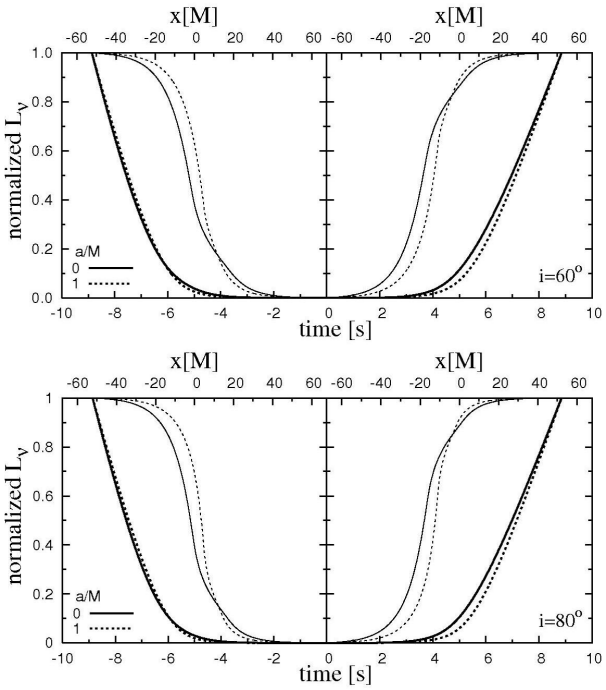

Fig. 6. Normalized light curves with (*thick lines*) and without (*thin lines*) the atmospheric effects of the companion star at observed energy of 1 keV for black hole spins $a/M = 0$ (*solid lines*) and 1 (*dotted lines*), and the observed inclination angles with respect to the rotation axis of the accretion disc $i = 60°$ (*top panels*) and $80°$ (*bottom panels*).

eclipsing light curves observed by the wavelength where the atmospheric absorption is effective.

5. Concluding Remarks

In this paper, we propose an eclipsing light-curve diagnosis for accretion flows around rotating black holes. When emission from an inner part of the accretion disc around black hole is occulted by a companion star, the light curves at ingress and egress show the asymmetric features due to the relativistic effects such as Doppler boosting originally pointed out by Fukue (1987). We show that the eclipsing light curves without the atmospheric effects clearly reflect the effects of the black hole's rotation. We also investigate the eclipsing light curves with the atmospheric effects of the companion star. Based on the adopted atmospheric model, after evaluating the absorption and scattering effects in X-ray, we calculate the images of the black hole shadows, the normalized light curves. Since the size of the most luminous parts of the accretion disc depends on the black hole spin, the crossing timescale of the companion star along the most luminous parts of the accretion disc can be one of the key physical quantities which distinguish the cases of rapidly rotating black holes and the cases of no rotating black hole.

In our calculations assuming the solar atmosphere, while the effects of black hole spins are negligible when the observed photon energy of 0.1 keV for both cases with no atmospheric effects and with atmospheric effects, for the observed photon energies of 1 keV and 10 keV the atmospheric absorption can not completely smeared out the difference between the cases of rapidly rotating black holes and the cases of no rotating black hole. However, these effects are smeared out by the atmospheric effects of the companion star at some fraction, and in our atmospheric model, the effects of the atmosphere are much larger than the effects of the black-hole spin. Therefore, even in the case that the light-curves contain the information of the black hole spin, it may be difficult to extract the information of the black hole spin if we do not have the realistic atmospheric profiles, such as, the temperature, the number densities for several elements. Even in such cases, based on our calculations, the light curve asymmetries due to the rotation of the accretion disc exist. Only when we have the reliable atmospheric model, in principle, the black hole spin can be determined from the eclipsing light curves observed around 1 keV. Takahashi & Watarai (2007) gives more information about these topics.

References

Bardeen, J.M., 1973, in Black Holes, ed. C. DeWitt and B. DeWitt (Gordon and Breach, New York)

Bardeen, J.M., Press, W.H., Teukolsky, S.A., 1972, ApJ, 178, 347

Cunningham, C. T., Bardeen, J. M., 1972, ApJ, 173, 137

Daw, A., DeLuca, E. E., Gould, L., 1995, ApJ, 453, 929

Fukue, J., 1987, Nature, 327, 600

Fukue, J., & Yokoyama, T., 1988, PASJ, 40, 15

Hirabayashi, H., et al., 2005, in Proc. 7th Symp. European VLBI Network on New Developments in VLBI Science and Technology, ed. R. Bachiller, F. Colomer, J.-F. Desmars, & P. de Vicente (Obs. Astron. Nac. Spain), 285 (astro-ph/0501020)

Junor, W., Biretta, J. A., Livio, M., 1999, Nature, 401, 891

Kato, S., Fukue, J., Mineshige, S., 1998, Black-Hole Accretion discs, Kyoto University Press

Shen, Z.-Q., Lo, K. Y., Liang, M.-C., Ho, P. T. P., Zhao, J.-H., 2005, Nature, 438, 62

Spitzer, L. Jr., 1978, Physical Processes in the Interstellar Medium, John Wiley & Sons, Inc.

Takahashi, R., 2004, ApJ, 611, 996

Takahashi, R., 2005, PASJ, 57, 273

Takahashi R., Watarai K. 2007 MNRAS, 374, 1515

Watarai, K., Takahashi, R., Fukue, J., 2005, PASJ, 57, 827

Watarai, K., Ohsuga, K., Takahashi, R., & Fukue, J., 2005, PASJ, 57, 513